MICROSTRUCTURAL CHARACTERIZATION OF IRRADIATED PWR STEELS USING THE ATOM PROBE FIELD-ION MICROSCOPE

M.K. Miller and M.G. Burke*

Metals and Ceramics Division, Oak Ridge National Laboratory, Oak Ridge, TN 37831-6376, USA.

*Department of Materials Science and Engineering, University of Pittsburgh, Pittsburgh, PA 15261, USA,
*present address Westinghouse R&D Center, Pittsburgh, PA 15235, USA.

ABSTRACT

Atom probe field-ion microscopy has been used to characterize the microstructure of a neutron-irradiated A533B pressure vessel steel weld. The atomic spatial resolution of this technique permits a complete structural and chemical description of the ultra-fine features that control the mechanical properties to be made. A variety of fine scale features including roughly spherical copper precipitates and clusters, spherical and rod-shaped molybdenum carbide and disc-shaped molybdenum nitride precipitates were observed to be inhomogeneously distributed in the ferrite. The copper content of the ferrite was substantially reduced from the nominal level. A thin film of molybdenum carbides and nitrides was observed on grain boundaries in addition to a coarse copper-manganese precipitate. Substantial enrichments of manganese and nickel were detected at the copper-manganese precipitate-ferrite interface and this enrichment extended into the ferrite. Enrichments of nickel, manganese and phosphorus were also measured at grain boundaries.

INTRODUCTION

The mechanical properties of the pressure vessel of a light water nuclear reactor change during in-service irradiation because of an embrittlement process. It has been shown statistically that this embrittlement is associated with low levels of copper and phosphorus in the steel. More recently, nickel and manganese were also shown to have a significant effect.[1] The most important aspect in understanding the embrittlement process is to perform a complete characterization of the microstructural evolution during service because it is the microstructure which determines the mechanical properties of these steels.

The ultra-fine features that are associated with the embrittlement process preclude direct observation by conventional techniques such as analytical electron microscopy and optical microscopy. The atom probe field-ion microscope (APFIM) with its inherent atomic spatial resolution is very suitable for this type of microstructural characterization. This instrument combines the atomic resolution imaging capability of the field-ion microscope with single atom chemical identification in a time-of-flight mass spectrometer and therefore provides both spatial and chemical characterization of the microstructure.

The APFIM has been successfully applied to characterize several model alloys and pressure vessel steels[2-5]. A high density of fine structural imperfections was observed in an Fe-0.34% Cu alloy after neutron irradiation at 288°C.[6] It was suggested that these imperfections were copper-stabilized microvoids; however, this was not substantiated by any experimental evidence. In an examination of unirradiated A533B-type steel weld, Worrall and Smith were unable to detect any copper or nickel clustering.[7] Examination of an Fe-0.6 at.% Cu binary alloy after aging at 500°C for 100 h revealed the presence of some copper-rich precipitates. In addition, no copper segregation to grain boundaries was detected in their study.

The effects of neutron irradiation on the microstructure of an A302B pressure vessel steel surveillance sample have been investigated by Miller et al.[2,4] The atom probe detected, for the first time, small copper-rich and phosphorus-rich regions, and the precipitation of small rod-shaped and spherical molybdenum carbides in the ferrite matrix. This study also revealed segregation of various solutes, other than copper and phosphorus, to ferrite-ferrite and ferrite-cementite interfaces. Small copper clusters that were enriched in nickel and manganese were observed in neutron-irradiated modified A533B pressure vessel steel weld metal by Burke et al.[3,5]

Recently, the microstructure in a series of model Fe-Cu-Ni-P-C steels has been characterized after neutron irradiation and thermal aging.[8] A high density of small, roughly spherical or disc-shaped copper clusters/precipitates were observed in the neutron-irradiated alloys that contained copper. Small spherical phosphorus clusters were observed in the irradiated copper-free alloys, and copper phosphides were observed in a high phosphorus Fe-Cu-Ni-P alloy. None of these clusters or precipitates were observed in thermally aged materials. The increases in the tensile and yield strengths that were observed after neutron irradiation resulted from the formation of these clusters and other lattice defects.

In this paper, an APFIM characterization of the fine-scale microstructure of an A533B pressure vessel steel weld after both neutron irradiation and thermal annealing at the irradiation temperature is presented.

EXPERIMENTAL

A schematic diagram of an atom probe field-ion microscope is shown in Fig. 1. Modern atom probes incorporate several instruments into a single vacuum system to enable a variety of types of analyses to be performed on a wide range of metallic and other materials.[9] In the instrument depicted in Fig. 1, four distinct instruments are available 1) a field-ion microscope (FIM), 2) an energy-compensated time-of-flight atom probe (ECTOFAP), 3) an imaging atom probe (IAP), and 4) a pulsed laser atom probe (PLAP). High resolution images of the specimen are obtained in the FIM. The ECTOFAP is used to fully quantify the chemistry of features observed in the FIM. Atomic resolution maps of a single element over the entire specimen surface may be obtained with the IAP to reveal variations in local chemistry. Unfortunately, the data obtained in the IAP is only semi-quantifiable. The PLAP is employed primarily for semiconducting materials and is therefore not pertinent to this investigation.

The energy-compensated variant of the atom probe has two major advantages over the older straight time-of-flight atom probe in that it substantially improves the mass resolution of the instrument by a factor of 10 to 20 times and it enables analyses to be performed while viewing the field-ion image. The improved mass resolution enables adjacent isotopes to be fully resolved, and therefore obtain more accurate compositional information. This is especially important in ferritic steels where many adjacent elements are present in relatively small quantities. The ability to view the microstructure while performing the chemical analysis has several benefits. It improves the spatial accuracy of the analysis and it dramatically reduces the time required to characterize the material. This permits the analysis of precipitates or other features that are present at a relatively low number densities. Also, the statistical significance of the APFIM analyses of features present at higher number densities is improved.

In this investigation, all APFIM analyses were performed in the ORNL energy-compensated instrument. A detailed description of this instrument can be found elsewhere.[10] The atom probe analyses were performed with a specimen temperature of 50-60K and with a pulse fraction of 20%. Field-ion specimens were electropolished using standard procedures[9] from blanks that were cut from miniature Charpy V-notch specimens.[11] All compositions are quoted in atomic percent.

Thin-foil transmission electron microscope specimens of the thermally aged material were examined in a JEOL 200CX operated at 200 kV.

The nominal composition of the A533B-type submerged arc pressure vessel steel weld[11] used in this study is given in Table 1. The weld was stress-relieved for 50h at 620°C and then irradiated to a neutron fluence of $1x10^{19}cm^{-2}$ (E>1MeV) in the University of Virginia reactor at 288°C for approximately 1 year. Unirradiated control material thermally aged for 556h at 288°C was also examined for comparison.

RESULTS AND DISCUSSION

TEM examination of thin-foil specimens revealed the presence of a variety of precipitates and inclusions in the ferrite matrix, Fig. 2. Ultra-fine features were characterized from both field-ion micrographs and atom probe chemical analyses. The distribution of second phase precipitates within the ferrite matrix was observed to be inhomogeneous for all the features described below.

Several coarse Mo_2C (~50 nm) precipitates that probably formed during the stress relief were observed in the APFIM. The Mo_2C imaged brightly with respect to the ferrite matrix, as shown in Fig. 3. The composition of the precipitate as determined by atom probe analysis is presented in Table 2. A significant enrichment of phosphorus to the carbide/ferrite interface was measured.

In addition to the coarse Mo_2C, ultra-fine (~1 nm) molybdenum carbides and nitrides were observed in the ferrite matrix of the irradiated material, Fig. 4. The molybdenum carbides were either spherical or rod-shaped while the molybdenum nitrides had a disc-like morphology. The extremely small size of these discrete precipitates made quantification of their chemistry difficult, although it is probable that large deviations from the equilibrium stoichiometric composition existed. APFIM analysis indicated that phosphorus was frequently associated with these precipitates. This ultra-fine precipitation in the matrix was not observed in the thermally aged control material. Both the coarse Mo_2C and the ultra-fine molybdenum carbides and nitrides were also observed in a previous APFIM characterization of A302B steel.[2]

Extremely fine (<1 nm), roughly spherical or disc-shaped darkly-imaging regions were observed in the field-ion images of the irradiated weld metal, Fig. 5. Atom probe composition profiles through these regions revealed a complex chemistry, Fig. 6. These zones were enriched in copper, nickel, manganese and silicon. The extent of the composition profiles for nickel and manganese indicated that the enrichment of these elements extended over a slightly larger distance into the ferrite as compared to the copper profile. It was not possible to unequivocally identify these regions as precipitates or clusters due to their ultra-fine size and diffuse nature; however, it should be emphasized that at this size scale, the distinction between a cluster and a precipitate is largely a matter of semantics. Phosphorus was detected in a high proportion of these zones. These features were only observed in the irradiated weld metal confirming that their formation was irradiation-induced. These types of copper-enriched features have been observed in both the A302B[2,4] and A533B materials[3,5], and the observation of enrichment of manganese and nickel is in agreement with the previous characterization of A533B welds[3,5]. The present study indicates that silicon also may have a role in the formation of the clusters/precipitates since a 10 fold enrichment of silicon was measured in these zones.

Atom probe analysis of the ferrite matrix revealed that the copper content was considerably lower in the irradiated material than the nominal value, Table 3, in agreement with the APFIM observations of the copper-enriched zones. It should be noted that the thermal mobility of copper at the irradiation temperature of 288°C is minimal, so that another mechanism should be invoked to explain the formation of these zones.[12] Some copper depletion in the thermal control material was also observed, consistent with precipitation during the stress relief treatment.

A coarse, darkly-imaging precipitate was observed on one side of a ferrite grain boundary, as shown in Fig. 7. The composition of this precipitate as determined by APFIM is given in Table 4. Although this copper-rich precipitate contained a substantial amount of manganese, this chemistry is still within the α copper single-phase field. A composition profile taken from the center of the copper precipitate into the ferrite matrix revealed significant enrichments of manganese and nickel at the interface, Fig. 8. The enrichment of nickel at the interface was 8.7 times the measured nickel content of the ferrite and 3.3 times that of the precipitate. Similarly, the values of manganese enrichment factors at the interface were 27.0 and 2.5 with respect to the measured manganese composition of the ferrite and precipitate, respectively. The size of this large precipitate suggests that it was formed during the stress-relief treatment.

In both the irradiated and the thermally aged materials, ferrite-ferrite grain boundaries, including the one shown in Fig. 7., were found to be decorated with a brightly-imaging, nearly continuous film. Atom probe analyses revealed that this film consisted of a mixture of molybdenum carbides and nitrides. This brightly-imaging film was similar to that observed at ferrite-ferrite and ferrite-cementite boundaries in the A302B investigation.[2,4] Nickel, manganese and phosphorus enrichments were detected at the ferrite grain boundaries for both irradiated and thermally aged conditions. The enrichment factors are presented in Table 5. While the nickel and manganese enrichments were similar for the irradiated and thermally aged welds, a significant difference was observed for phosphorus in that the irradiated material exhibited enhanced segregation. These results are in agreement with previous Auger results on thermally aged A533B steel which also provided evidence of phosphorus segregation to grain boundaries.[13]

CONCLUSIONS

The complex and diverse reactions occurring in neutron-irradiated A533B PWR steel welds have been characterized by APFIM. The extremely fine scale of the features detected in these welds necessitates the use of the atomic resolution of the APFIM technique since it would be difficult, if not impossible, to characterize the microstructure by other techniques. The multi-element chemistry of the ultra-fine irradiation-induced zones and precipitates clearly demonstrates the importance of examining actual reactor materials to elucidate the roles of manganese,

nickel, silicon, and phosphorus in the embrittlement process.

Acknowledgment

The authors would like to thank Professors G.R. Odette and G.E. Lucas of the University of California - Santa Barbara for helpful discussions and for supplying the material used in this round robin investigation, and K.F. Russell for her technical assistance. This research was sponsored by the Division of Materials Sciences, U.S. Department of Energy, under contract DE-AC05-84OR21400 with Martin Marietta Energy Systems, Inc. and through the SHaRE program under contract DE-AC05-76ORO0033 with Oak Ridge Associated Universities.

REFERENCES

[1] S.P. Grant and S.L. Earp, in "Effects of Radiation on Materials, ASTM STP 870, eds. F.A. Garner and J.S. Perrin (1985) ASTM, Philadelphia, pps. 1027-1045.

[2] M.K. Miller and S.S. Brenner, Res Mechanica, 10 (1984) 161-168.

[3] M.G. Burke and S.S. Brenner, J. de Physique, 47-C2 (1986) 239-244.

[4] M.K. Miller, J.A. Spitznagel, S.S. Brenner and M.G. Burke, Proc. 2nd. Int. Sym. on Environmental Degradation of Materials in Nuclear Power Systems - Water Reactors, Monterey 1985, eds. J.T.A. Robert, J.R. Weeks, and G. Theus, American Nuclear Society, pp. 523-528.

[5] S.P. Grant, S.L. Earp, S.S. Brenner and M.G. Burke, Proc. 2nd. Int. Sym. on Environmental Degradation of Materials in Nuclear Power Systems - Water Reactors, Monterey 1985, eds. J.T.A. Robert, J.R. Weeks, and G. Theus, American Nuclear Society, pp. 385-392.

[6] S.S. Brenner, R. Wagner and J.A. Spitznagel, Met. Trans., 9A (1978) 1761-1764.

[7] G.M. Worrall and G.D.W. Smith, J. de Physique, 47-C2 (1986) 245-250.

[8] M.K. Miller, F. Ebrahimi, D.T. Hoelzer, J.R. Hawthorne and M.G. Burke, J. de Physique, (1987) in press.

[9] M.K. Miller, Int. Met. Rev., 32 No.5, (1987) in press.

[10] M.K. Miller, J. de Physique, 47-C2 (1986) 493-498; 47-C2 (1986) 499-504.

[11] G.R. Odette and G.E. Lucas, 1987, EPRI final report No. RP1021-7.

[12] S.B. Fisher, J.E. Harbottle and N.B. Aldridge, "Dimensional stability and mechanical behaviour of irradiated metals and alloys", Brighton, 1985, pub. British Nuclear Energy Society, London.

[13] S.G. Druce, G. Gage and G. Jordan, Acta Metall., 34 (1986) 641-652.

Table 1. Nominal composition of the A533B weld[11]

Element	wt. %	at. %
Carbon	0.12	0.55
Copper	0.4	0.35
Nickel	0.6	0.57
Manganese	1.36	1.37
Molybdenum	0.44	0.25
Silicon	0.51	1.01
Chromium	0.044	0.047
Phosphorus	0.006	0.011
Sulphur	0.013	0.022
Iron	balance	balance

Table 2. Atom probe analysis of a coarse Mo_2C precipitate

Element	Composition (at. %)
Molybdenum	63.6 ± 1.4
Carbon	31.4 ± 1.4
Iron	2.4 ± 0.4
Manganese	2.1 ± 0.4
Phosphorus	0.09 ± 0.09
Oxygen	0.26 ± 0.15
Nitrogen	0.17 ± 0.12

Table 3. Atom probe composition of the ferrite matrix (at. %).

Element	Irradiated	Thermal Control
Carbon	0.01	0.03
Copper	0.06	0.11
Nickel	0.75	0.53
Manganese	1.23	1.31
Molybdenum	0.12	0.28
Silicon	0.98	1.19
Chromium	0.04	0.03
Phosphorus	0.005	0.015
Sulphur	0	0
Iron	balance	balance

Table 4. Atom probe analysis of a grain boundary copper-manganese precipitate.

Element	Composition (at. %)
Copper	83.6 ± 1.2
Manganese	14.6 ± 1.1
Nickel	1.5 ± 0.4
Iron	0.3 ± 0.2

Table 5. Grain Boundary Enrichment Factors with respect to the ferrite composition

	Ni	Mn	P
Irradiated	2.2	1.6	12.5
Thermal	1.6	2.1	3.6

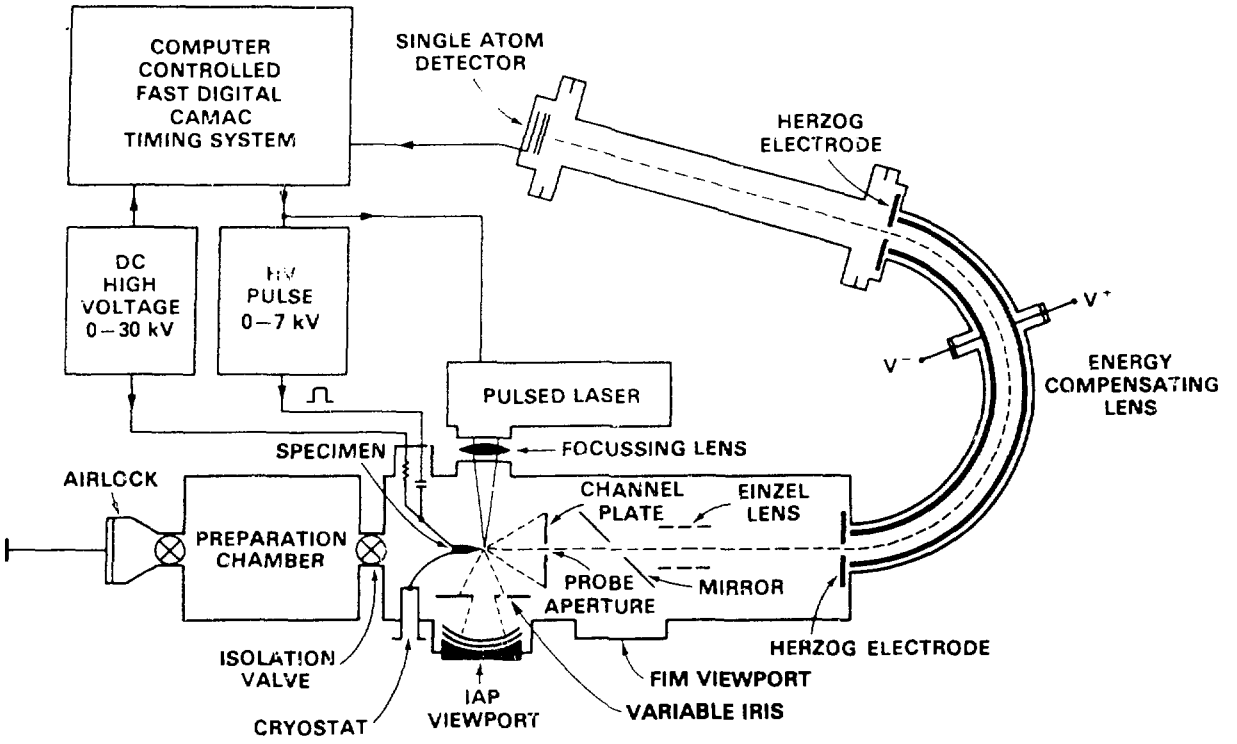

Fig. 1. Schematic diagram of an atom probe field-ion microscope

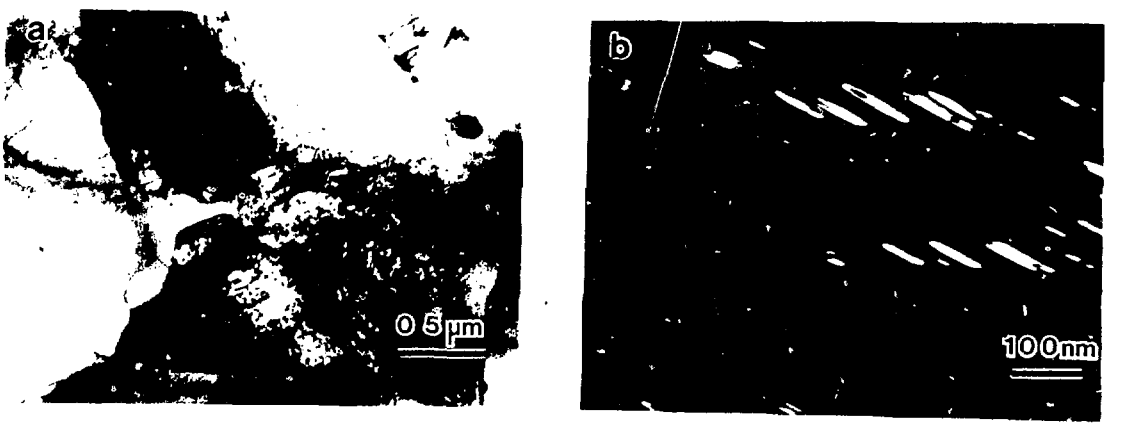

Fig. 2. Transmission electron micrographs of thermally aged A533B weld steel showing a) general ferritic microstructure and b) carbide precipitates.

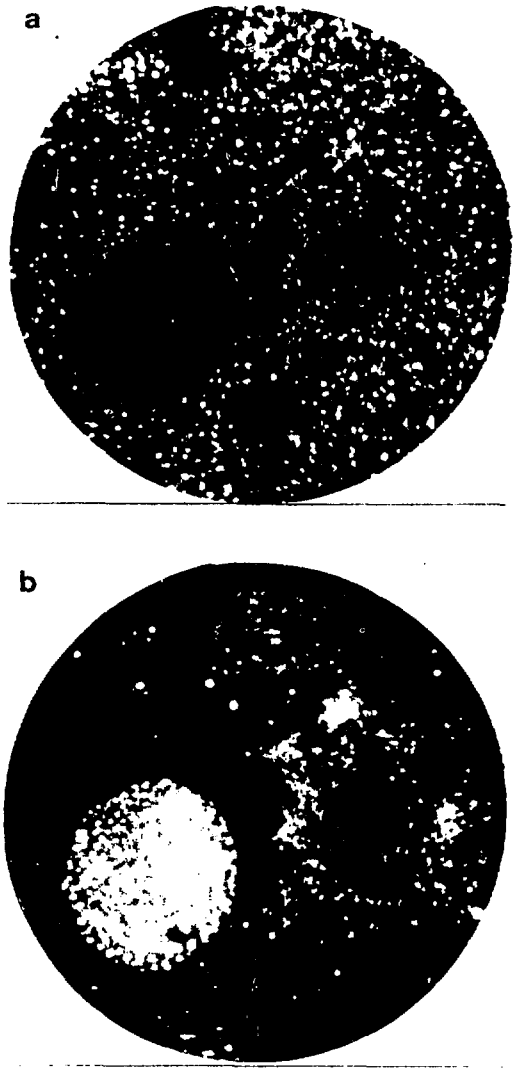

Fig. 3. Field-ion micrographs of a coarse Mo_2C carbide in the irradiated material a) at best image voltage for ferrite matrix and b) at best image voltage for precipitate.

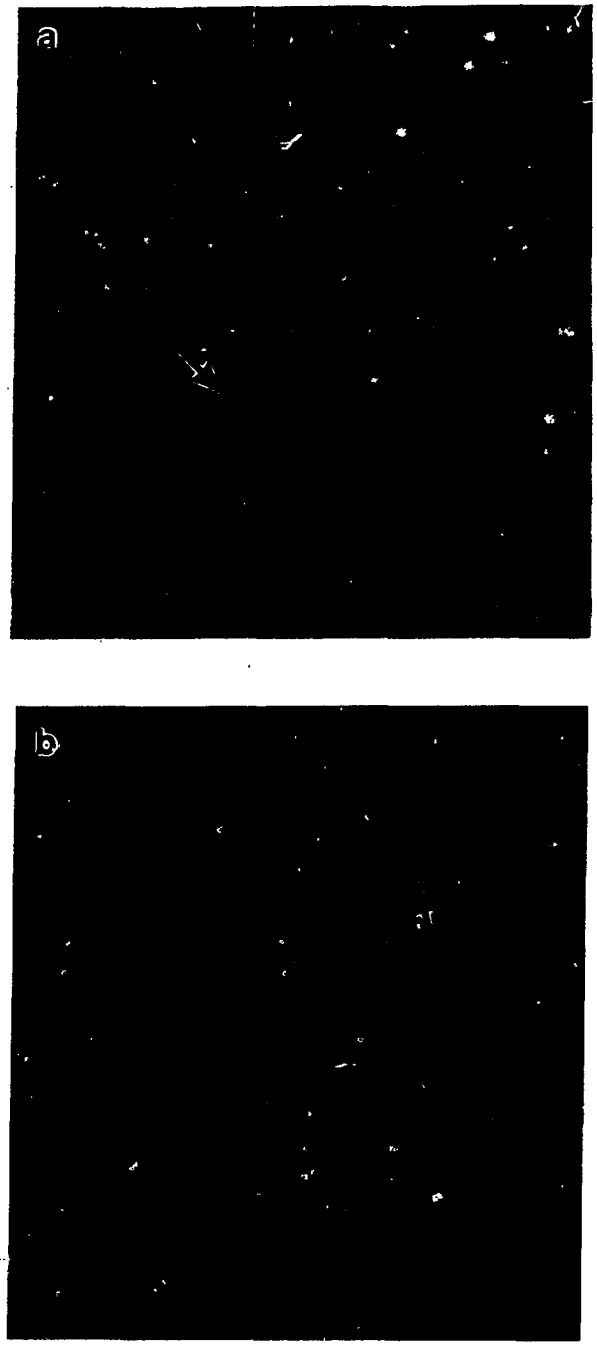

Fig. 4. Field-ion micrographs of irradiated material showing a) ultra-fine molybdenum carbides and b) disc-shaped molybdenum nitride.

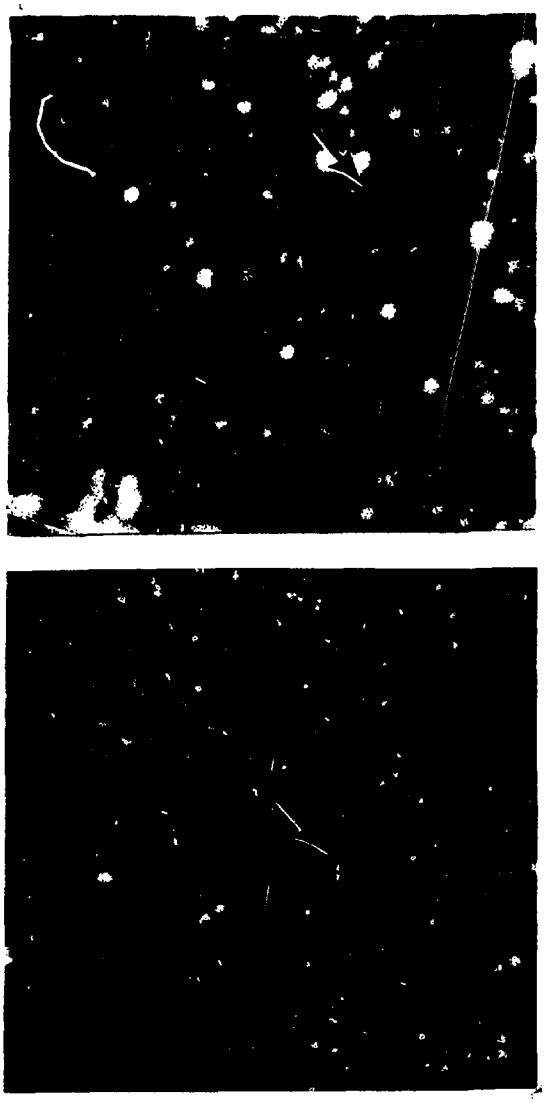

Fig. 5. Field-ion micrographs of small darkly-imaging copper-enriched zones in irradiated material.

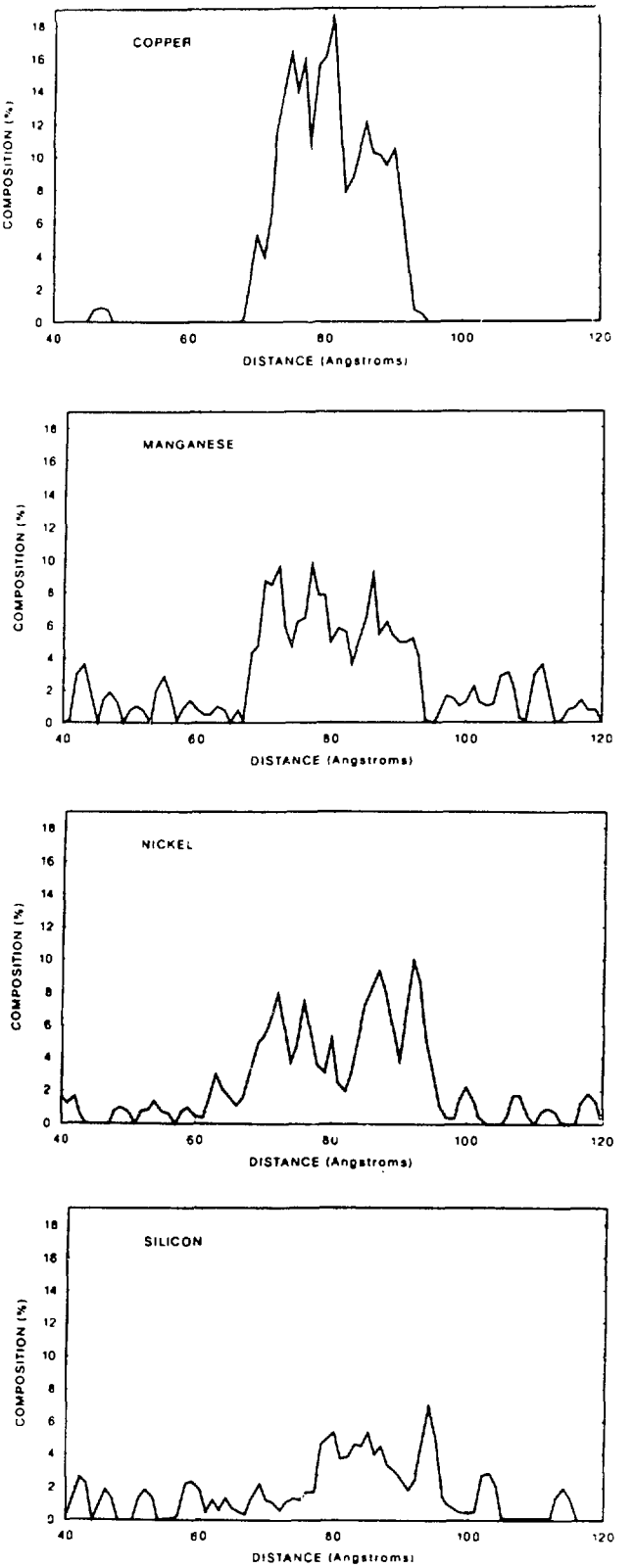

Fig. 6. Atom probe composition profiles through a copper-enriched zone in irradiated material.

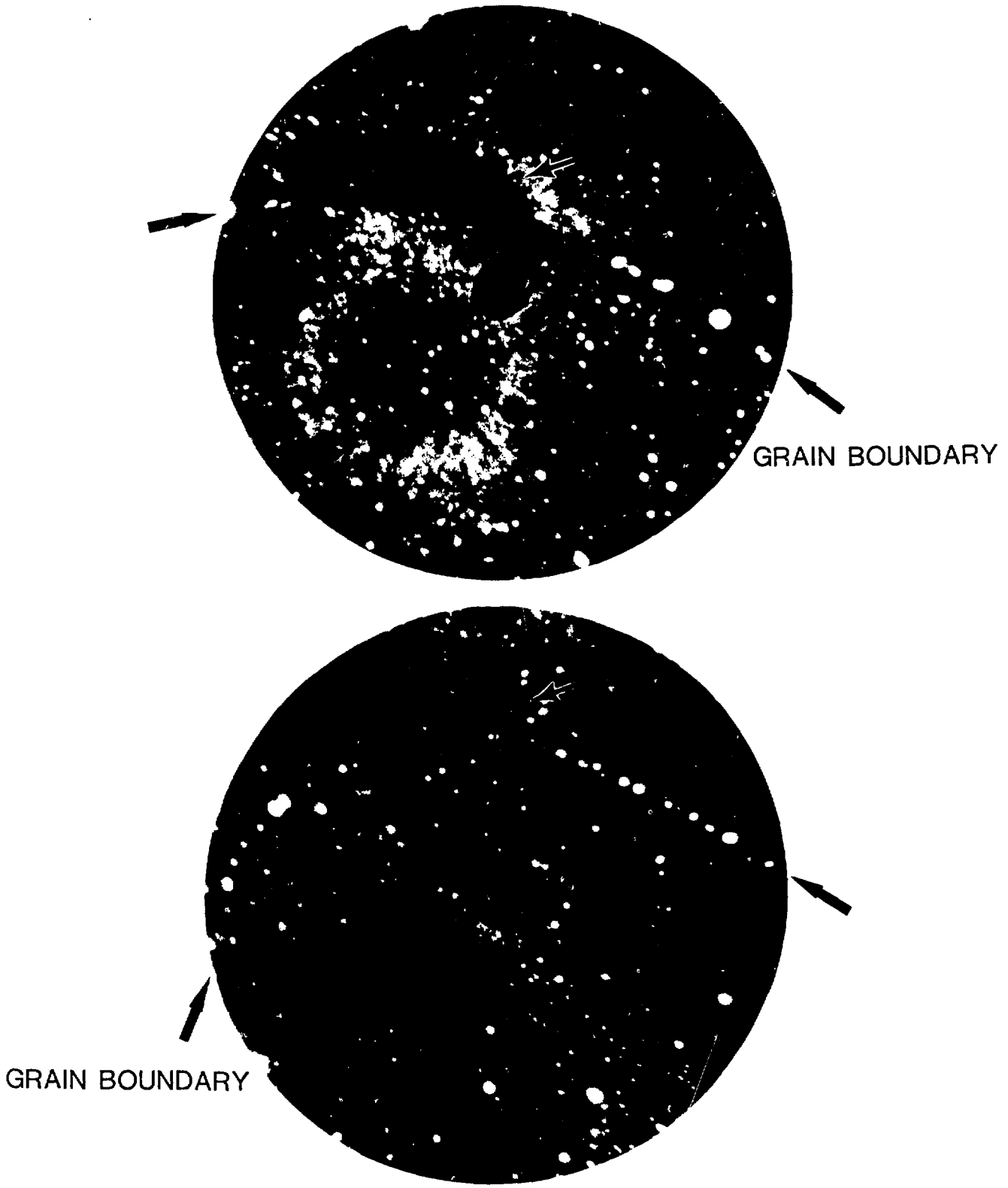

Fig. 7. Field-ion micrographs at different intervals of field-evaporation of a coarse darkly-imaging copper-manganese precipitate on a ferrite grain boundary. The ferrite-ferrite grain boundary was decorated with a thin brightly-imaging film of molybdenum carbides and nitrides.

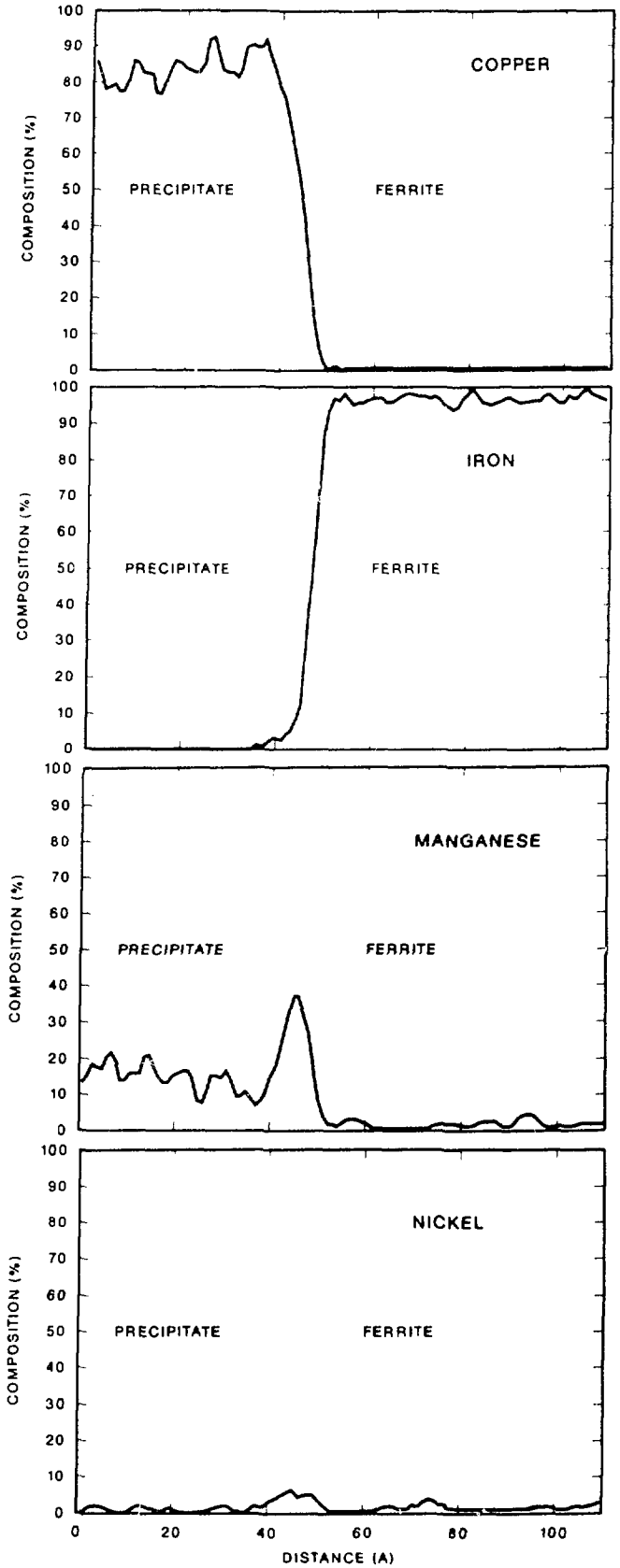

Fig. 8. Atom probe composition profile through the copper-manganese precipitate shown in Fig. 7 into the ferrite matrix.